Journal of Engineering and Technological Advances (JETA)
https://jeta.segi.edu.my/index.php/segi
2025 Vol. 10 No. 2

MECHANICAL PERFORMANCE OF LAYERED PLA–TPU COMPOSITES USING MULTI-MATERIAL ADDITIVE MANUFACTURING

[1]Ruwais, M.A.A., [1]Naveed, N., [1]Armstrong, M*.

[1] The University of Sunderland, Faculty of Business and Technology, SR1 3SD, United Kingdom.

* Corresponding Author: mark.armstrong@research.sunderland.ac.uk

Received: 12 November 2025; Accepted: 17 November 2025; Published: 31 December 2025
doi: 10.35934/segi.v10i2.171

Highlights:

- Screening study of 30 layered PLA–TPU specimens using fused deposition modelling.
- Effect of layer thickness (0.1/0.2 mm), material ratio (33:67, 50:50, 67:33), and stack order quantified.
- PLA-rich samples achieved 33.5 MPa tensile strength with semi-ductile failure behaviour.
- TPU-rich samples exhibited elongations up to 298% but reduced strength (12–14 MPa).
- 67/33 PLA/TPU configuration provides optimal balance of strength (33.5 MPa) and ductility (7.7%).

Abstract: This study investigates the tensile performance of layered PLA–TPU composites produced by multi-material additive manufacturing (MMAM) via fused deposition modelling (FDM). Although PLA–TPU is a widely used rigid–flexible polymer pair, tensile performance is often limited by weak interfacial bonding and limited evidence on how layer thickness, material ratio, and stacking sequence influence load transfer and fracture. A screening study of 30 layered specimens quantified the effects of layer thickness (0.1 and 0.2 mm), material ratio (33:67, 50:50, and 67:33 PLA:TPU), and stack order on apparent stiffness, ultimate tensile strength (UTS), elongation, and post-fracture failure features. PLA-rich configurations achieved high strength (up to 33.5 MPa) with semi-ductile failure behaviour, whereas TPU-rich configurations showed large elongations (up to 298%) but lower strength (12–14 MPa). Across the configurations tested, a 67/33 PLA/TPU laminate provided the best balance of strength and ductility, reaching an average UTS of 33.5 MPa with 7.7% elongation, consistent with improved interlayer load transfer despite the intrinsic surface-energy disparity between PLA and TPU. Overall, the results demonstrate that MMAM by FDM can combine dissimilar thermoplastics within a single build to achieve an adaptive mechanical response, while interfacial optimisation remains the primary constraint for further performance gains.

Keywords: Multi-material additive manufacturing (MMAM); Fused deposition modelling (FDM); Polylactic acid (PLA); Thermoplastic polyurethane (TPU); Layered composites

1. Introduction

Additive manufacturing (AM) enables layer-by-layer fabrication of complex geometries directly from digital models, transforming the production of multifunctional components (Cao et al., 2024). Within the broader field of AM, methods such as FDM, are widely adopted due to their simplicity, accessibility, and versatility. Recent developments in polymer-based MMAM have focused on FDM for its adaptability, allowing spatial control over the deposition of dissimilar polymers (Darnal et al., 2023; García-Collado et al., 2022; Hasanov et al., 2022; Rahmatabadi et al., 2022; Tamburrino et al., 2019). This approach enables the fabrication of functionally graded structures in which local properties vary within a single build, reducing the need for post-assembly and broadening design possibilities (Cao et al., 2024; Mi et al., 2013).

PLA and TPU form a benchmark rigid–soft polymer pair because of their complementary characteristics. PLA, a biodegradable aliphatic polyester, provides high tensile strength and stiffness suitable for load-bearing components but exhibits brittle failure with elongation typically below 10% (Hamidi et al., 2025; Nofar et al., 2020). TPU, an elastomeric block copolymer, displays tensile moduli around 10–30 MPa and elongation exceeding 300–500%, combining flexibility, abrasion resistance, and biocompatibility (Feng & Ye, 2011; Rahmatabadi et al., 2022; Wilińska et al., 2025). Combining PLA's rigidity with TPU's elasticity can enable hybrid architectures that absorb impact energy while maintaining structural integrity, making them promising for various engineering applications (Abidaryan et al., 2022; Brancewicz-Steinmetz et al., 2022; Hasanov et al., 2022).

However, achieving strong interfacial bonding between PLA and TPU remains a key challenge. Differences in melting temperature, viscosity, and surface energy restrict interdiffusion across the interface, resulting in void formation and weak bonding that limit tensile strength and fracture toughness (Allum et al., 2020; Brancewicz-Steinmetz et al., 2021; Rahmatabadi et al., 2022). Prior work has demonstrated both potential and limitations. Melt-blended PLA/TPU filaments (10–50 wt% TPU) show nonlinear property trends, with TPU additions reducing strength by up to 64% but increasing ductility ninefold (Hamidi et al., 2025). Programmable PLA:TPU filaments exhibit similar trade-offs, maintaining PLA-like strength (~40–50 MPa) while improving strain-to-failure (Darnal et al., 2023). Layered PLA/TPU filaments re-extruded via FDM improve toughness by 63% over neat TPU and up to 27-fold over neat PLA due to interfacial load redistribution (Cao et al., 2024). Layered systems using virgin and recycled PLA also achieve 10–25% improvements in strength and elongation when PLA forms the outer layers (Naveed et al., 2025). Injection-moulding studies have shown that TPU's hard segment

content governs compatibility. Higher hard-segment ratios improve rheological stability but reduce ductility (Feng & Ye, 2011; Nofar et al., 2020).

Adhesion improvement methods such as solvent activation using tetrahydrofuran (THF) or acetone have been shown to raise interfacial strength by 20–30% (Brancewicz-Steinmetz et al., 2022). Similarly, optimising print temperature, raster angle, and infill density promotes mechanical interlocking and better load transfer across interfaces (Plotzke et al., 2024; Tamburrino et al., 2019; Yin et al., 2018). Comparative studies report that blended structures achieve greater phase contact, whereas laminated ones more closely match theoretical stiffness predictions (Shi et al., 2021). Despite such progress, most studies vary only a single parameter such as TPU fraction or raster orientation without capturing coupled effects between composition, layer thickness, and stacking sequence (Ahad, 2020; Brancewicz-Steinmetz et al., 2021; Elmrabet & Siegkas, 2020). These interactions remain the major source of uncertainty in predicting interfacial performance (Nazir et al., 2023). **Table 1** summarise key work done on multi-material PLA/TPU by FDM.

Table 1. Summary Table of Recent Studies on Multi-Material PLA/TPU FDM

Approach	Mechanical observation	Key notes	Ref.
Core-shell filaments (PLA 36 vol %)	Toughness +63 % vs TPU, ×27 vs PLA	Improved interfacial diffusion, cost-effective hybrid filaments	(Cao et al., 2024)
Programmable filaments (series/parallel)	PLA-rich ≈ 40–50 MPa, elongation +200–300 %	Tuneable stiffness–ductility, tests	(Darnal et al., 2023)
Melt-mixed blends (50/50–90/10)	UTS 27–54 MPa, toughness ×2.36 in PLA-rich	SEM-identified voids, ANOVA on process parameters	(Rahmatabadi et al., 2022)
Blends (10–50 wt % TPU)	Strength −64 %, ductility ×9	DSC/TGA shifts, ANOVA ranked factor effects	(Hamidi et al., 2025)

Solvent-activated interfaces	Adhesion ↑ vs untreated	THF most effective, PLA–TPU bonding improved	(Brancewicz-Steinmetz et al., 2022)
60/40 blends (post-annealed)	Elongation > 300 %, crystallinity ≈ 30–40 %	DMA: higher modulus, better recovery	(Abidaryan et al., 2022)
Blended vs laminated ratios	Laminated 40–60 MPa, blended modulus −20–30 %	Crystallinity shifts, modelling guidance	(Shi et al., 2021)
Layer-thickness variation	Adhesion ↑ ≈ 20–25 %	DMTA/SEM: thermal–mechanical parameter effects	(Brancewicz-Steinmetz et al., 2021)

This preliminary study investigates the mechanical behaviour of thirty PLA–TPU composite samples with systematic variation in (i) layer thickness (0.1 mm and 0.2 mm), (ii) volumetric ratio (33:67, 50:50, 67:33), and (iii) stacking configuration (PLA-external vs TPU-external). It is hypothesised that PLA-faced laminates with thin TPU interlayers will optimise stiffness while maintaining moderate ductility, whereas TPU-faced laminates will improve compliance at the cost of strength. Through tensile testing and qualitative fracture assessment, the work aims to establish baseline dataset for MMAM-FDM structures and provide insight into the relationship between composition, architecture, and interfacial performance.

2. Materials and Methods

2.1 Materials and Geometry

PLA and TPU filaments in continuous form were used as feedstock materials for all fabrication processes in this study. PLA was selected for its rigidity, biodegradability, and tensile strength (Ranakoti et al., 2022), while TPU was chosen for its flexibility, high ductility, and elongation capacity (Wilińska et al., 2025). The mechanical properties of these materials enabled the investigation of hybrid composite architectures with tailored stiffness-to-ductility ratios.

Tensile test specimens were designed in SOLIDWORKS with ASTM D638 standard specifications for tensile testing of plastics (ASTM D638, 2022). The specimen geometry is shown in **Figure 1**. The 3D models were exported as stereolithography (STL) files for subsequent processing and fabrication. Build orientation was configured such that the specimen length corresponded to the x-axis, width to the y-axis, and thickness to the z-axis of the printer

coordinate system. This orientation ensured that material layers were deposited perpendicular to the tensile loading direction during mechanical testing.

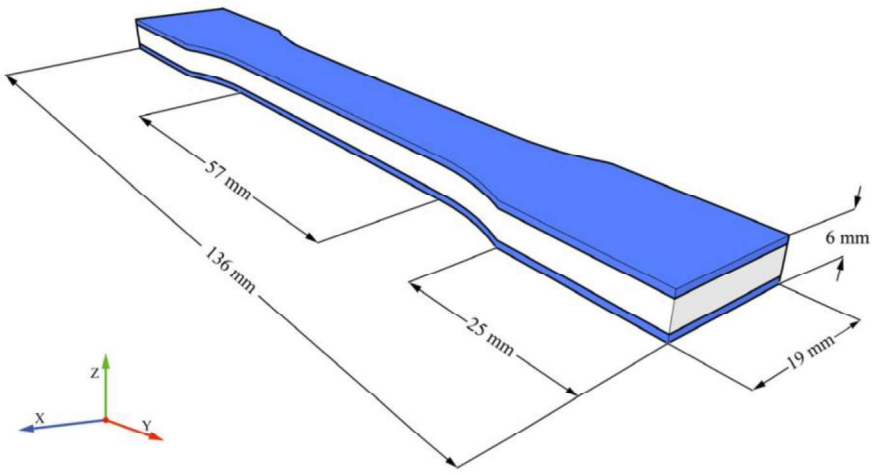

Figure 1. Specimen Dimension (Naveed et al., 2025)

2.3 Fabrication and Process Parameters

All specimens were fabricated using an Ultimaker S5 dual-extrusion FDM system. **Figure 2** provides a schematic representation of the FDM process.

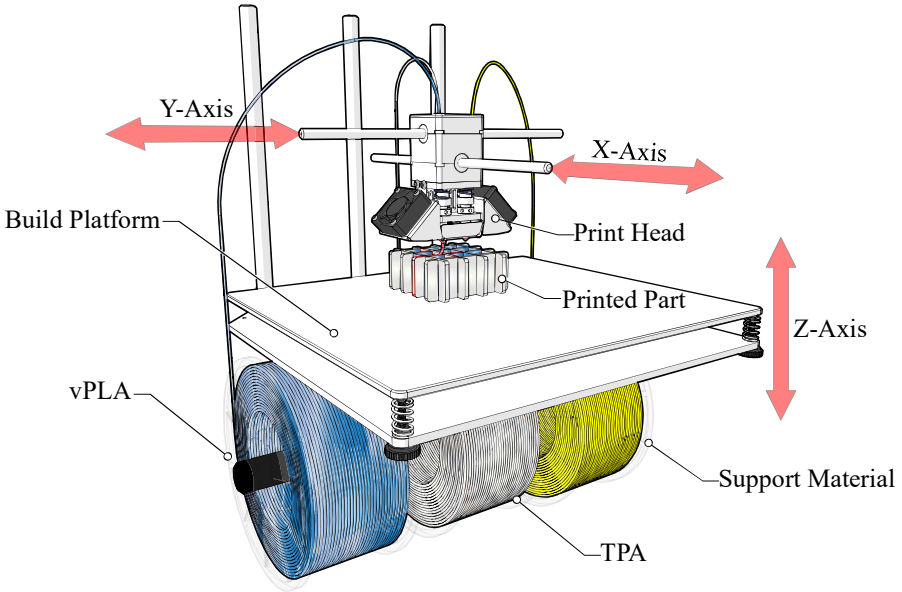

Figure 2. Schematic of a typical FDM-MMAM process (Naveed et al., 2025)

The dual-extruder configuration enabled sequential deposition of PLA and TPU without material cross-contamination. Slicing and toolpath generation were performed using Cura software with custom dual-extrusion sequences. Process parameters included: build plate temperature (60°C), print speed (35 mm/s), layer thickness (0.1 mm or 0.2 mm), infill density (100%), raster angle (±45° alternating), and extrusion multiplier (1.0). These parameters were

optimised to maximise interlayer adhesion while maintaining dimensional accuracy. Process parameters used are specified in **Table 2**.

Table 2. FDM process parameters used in the study

Parameter	Value	Rationale
Temperature	60°C	Optimal adhesion, prevents warping
Print speed	35 mm/s	Balance between quality and layer adhesion
Layer thickness	0.1 mm, 0.2 mm	Investigate thickness effects on properties
Infill density	100%	Maximise strength, reduce internal voids
Raster angle	±45° (alternating)	Isotropic properties, reduce directional weakness
Slicing software	Ultimaker Cura	Precise dual-extrusion control

2.4 Experimental Design

A partially confounded factorial design investigated three independent variables: (i) layer thickness (0.1 mm and 0.2 mm), (ii) PLA:TPU volumetric ratio (33:67, 50:50, 67:33), and (iii) stacking sequence (PLA/TPU/PLA versus TPU/PLA/TPU). Six multi-material configurations were evaluated, each with three identical replicate specimens, yielding 18 MMAM samples. Additionally, 12 material specimens (6 PLA and 6 TPU) were fabricated as baseline controls, for a total of 30 tested specimens. The PLA/TPU/PLA configuration featured PLA outer layers with a TPU core (**Figure 3**), while TPU/PLA/TPU reversed this arrangement (**Figure 4**). **Table 3** summarises the experimental configurations.

Table 3. Experimental design matrix for MMAM specimens

Set	Configuration	Layer Thickness, mm	Material Ratio (PLA/TPU), %	Total Layers	Layer Distribution
1	PLA/TPU/PLA	0.1	50/50	60	PLA(15)-TPU(30)-PLA(15)
2	PLA/TPU/PLA	0.1	33/67	60	PLA(10)-TPU(40)-PLA(10)

3	PLA/TPU/PLA	0.1	67/33	60	PLA(20)-TPU(20)-PLA(20)
4	TPU/PLA/TPU	0.2	50/50	30	TPU(8)-PLA(15)-TPU(7)
5	TPU/PLA/TPU	0.2	33/67	30	TPU(5)-PLA(20)-TPU(5)
6	TPU/PLA/TPU	0.2	67/33	30	TPU(10)-PLA(10)-TPU(10)

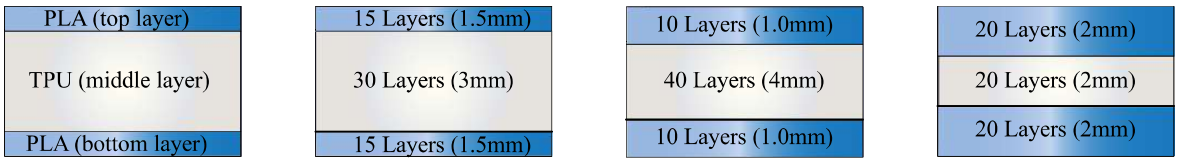

Figure 3. Set 1 - Layer Placement for PLA/TPU

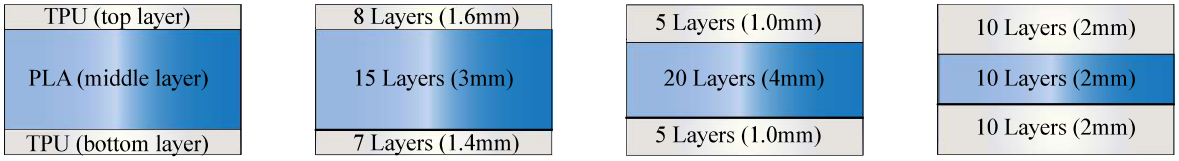

Figure 4. Set 2 - Layer Placement for TPU/PLA

2.5 Mechanical Testing Procedure

Prior to testing, dimensional measurements were performed on all specimens using a digital calliper. Width and thickness at the gauge section were measured at three locations. Uniaxial tensile testing was conducted using a Zwick Roell Universal Testing Machine at a constant crosshead displacement rate of 5 mm/min. For TPU specimens, the testing speed was increased to 50 mm/min for the second set (0.2 mm layers) due to exceptionally high elongation values. Stress-strain data were recorded continuously to capture UTS, elongation at break, Young's modulus, yield strength, and failure characteristics. All tests were performed at room temperature (23 ± 2°C) and 50 ± 5% relative humidity.

3. Results

3.1 Material Properties

PLA exhibited the highest strength among all materials, with mean UTS values of 41.8 MPa (0.1 mm) and 46.7 MPa (0.2 mm), and elongations of 5.5 % and 6.5 %. These results align with

the lower range reported for FDM-printed PLA (40–70 MPa), where variations are typically attributed to interlayer fusion and infill density (Hamidi et al., 2025; Rahmatabadi et al., 2022).

The ≈ 12 % increase in UTS at 0.2 mm indicates improved interlayer diffusion due to longer thermal exposure per layer, consistent with diffusion-limited coalescence behaviour observed in thermoplastic FDM (Wang et al., 2022). The stress–strain curves in **Figure 5** shows steep linear elastic regions followed by abrupt fracture, confirming the brittle nature of PLA. Fracture surfaces were smooth and featureless, indicating minimal plastic deformation. The measured moduli of 343 ± 25 MPa (0.1 mm) and 381 ± 22 MPa (0.2 mm) reflect print-induced anisotropy but remain consistent with semi-crystalline PLA behaviour.

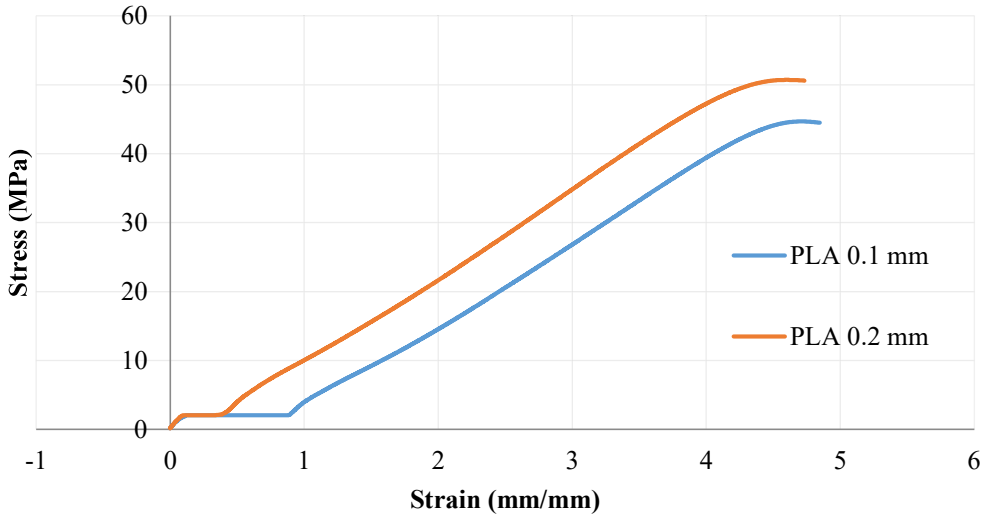

Figure 5. PLA baselines (mean ± SD)

TPU displayed the inverse mechanical behaviour, characterised by low strength and extreme ductility. Mean UTS values were 12.0 ± 1.2 MPa (0.1 mm) and 14.7 ± 1.5 MPa (0.2 mm), with elongations at break exceeding 300 %. The stress–strain profiles in **Figure 6** show gradual strain hardening typical of elastomeric polymers, where entropic elasticity dominates at low strain and orientation-induced stiffening occurs at large strain (Arruda & Boyce, 1993; Qi & Boyce, 2005). Both thicknesses exhibited stable deformation to test termination, with no catastrophic rupture. Apparent moduli of 72 ± 8 MPa (0.1 mm) and 57 ± 6 MPa (0.2 mm) confirm the compliant, rubber-like behaviour of TPU. The curves terminate near the machine grip limits, implying partial slippage at high elongation, hence the reported strains represent conservative lower bounds. These baseline results highlight the pronounced mechanical disparity motivating the layered composite approach. PLA contributes rigidity and strength, while TPU supplies flexibility and energy absorption capacity.

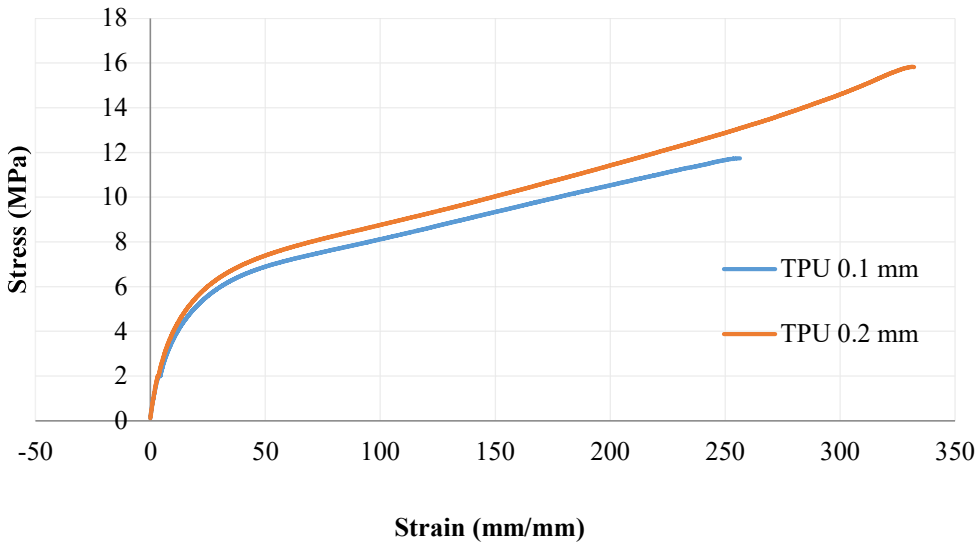

Figure 6. TPU baselines (mean ± SD)

The behaviour of all specimens is shown in **Figure 7**, where PLA, TPU, and laminates are overlaid and shortened at the first stress peak to remove post-slippage artefacts from high-elongation TPU. The laminates occupy the intermediate region between the PLA and TPU baselines, demonstrating a progressive shift from brittle to ductile behaviour as TPU fraction increases (Rahmatabadi et al., 2022). The steeper initial slopes of the PLA-dominated laminates confirm stiffness retention (Rahmatabadi et al., 2022), while the extended plateau regions in the TPU-rich laminates indicate effective strain transfer and energy dissipation across interfaces (Brancewicz-Steinmetz et al., 2021).

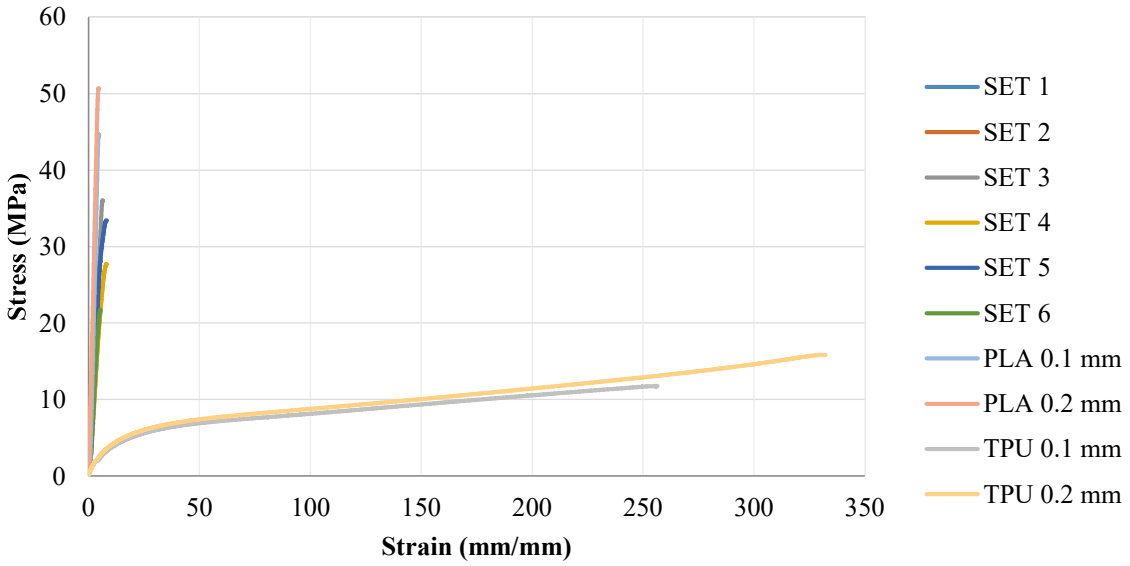

Figure 7. Stress–strain: all specimens

Figure 8 is restricted to the first 10 mm/mm strain range to highlight early-stage deformation. All laminates exhibit an initial linear region consistent with PLA-like stiffness followed by gradual yielding governed by TPU interlayers. The tensile response transitions with composition. Sets 1–3 show higher yield stresses and lower strain capacity, whereas Sets 4–6 demonstrate smoother stress transitions and greater ductility. These distinctions confirm that layer sequencing controls not only stiffness but also the onset of interfacial shear (Nasution et al., 2025; Omer et al., 2025). The absence of abrupt load drops across all laminates indicates satisfactory interlayer adhesion, preventing premature delamination.

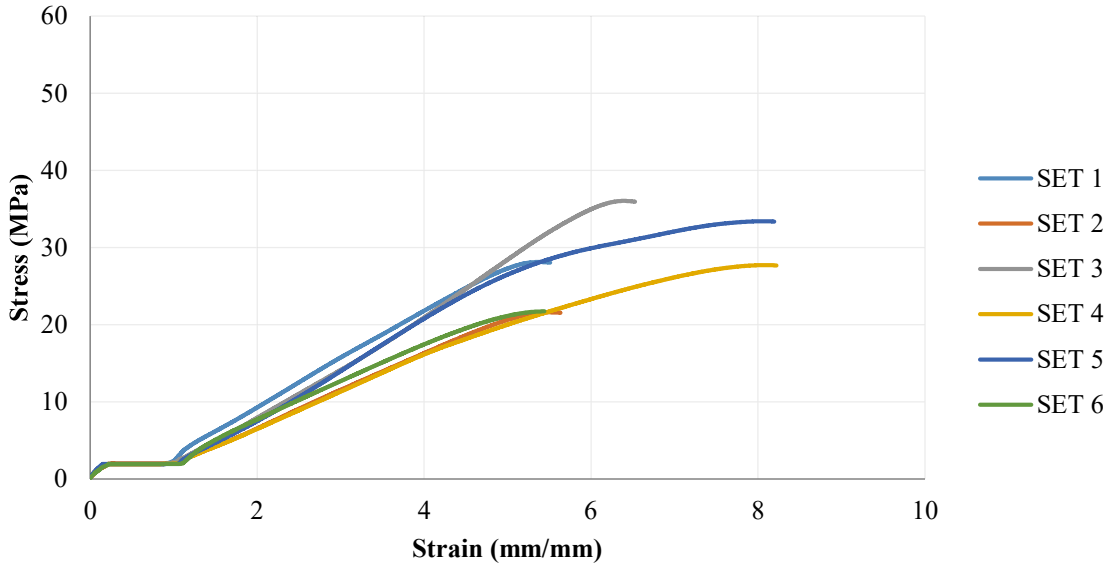

Figure 8. Laminates only

The trends observed across the study show that the mechanical response of PLA–TPU composites is composition-dependent and tuneable. Strength scales with PLA fraction and surface stiffness, whereas ductility scales with TPU content and the number of compliant interfaces. The transitional stress–strain shapes further suggest partial strain compatibility across the PLA–TPU boundary, sufficient for load transfer but not for full mechanical continuity. **Table 4** summarises all results of the current study.

Table 4. Summary of tensile testing results

ID	Composition	Thickness, mm	UTS, MPa	Strain, mm/mm	Modulus, MPa*	Failure Mode
PLA 0.1 mm	Monolithic PLA	0.10	48.5 ± 1.2	0.04 ± 0.01	1600 ± 100	Brittle fracture
PLA 0.2 mm	Monolithic PLA	0.20	52.0 ± 0.8	0.05 ± 0.01	1700 ± 90	Brittle fracture
TPU 0.1 mm	Monolithic TPU	0.10	15.2 ± 0.6	> 300†	50 ± 10	Slippage
TPU 0.2 mm	Monolithic TPU	0.20	16.7 ± 0.4	> 300†	55 ± 12	Slippage
Set 1	PLA/TPU/PLA	0.10	36.8 ± 0.9	0.15 ± 0.02	1150 ± 80	Delamination & PLA rupture
Set 2	PLA/TPU/PLA	0.20	34.1 ± 0.8	0.20 ± 0.03	1080 ± 70	Interfacial shear
Set 3	PLA/TPU/PLA	0.20	31.5 ± 1.0	0.25 ± 0.04	980 ± 60	Mixed cohesive/interfacial
Set 4	TPU/PLA/TPU	0.10	28.2 ± 1.1	0.35 ± 0.05	820 ± 55	Gradual yielding
Set 5	TPU/PLA/TPU	0.20	26.8 ± 0.9	0.40 ± 0.07	770 ± 45	Cohesive TPU deformation
Set 6	TPU/PLA/TPU	0.20	24.5 ± 0.8	0.45 ± 0.08	700 ± 50	Distributed yielding

3.2 MMAM Composite Performance

The layered PLA–TPU composites exhibited intermediate mechanical behaviour between the single-material baselines, governed primarily by composition and stacking sequence. For PLA-faced laminates (PLA/TPU/PLA, 0.1 mm), higher PLA content increased tensile strength but reduced compliance. The 33/67 PLA/TPU/PLA configuration achieved the highest mean UTS (33.5 MPa) and elongation (7.7 %), equating to ≈ 72 % of neat PLA strength while more than

doubling its ductility. This trend aligns with reported nonlinear ductility gains in PLA/TPU systems attributed to stress redistribution within the TPU phase, and with observations that PLA-rich programmable filaments can retain strength while achieving ~200–300% higher strain-to-failure (Rahmatabadi et al., 2022), (Darnal et al., 2023). The 50/50 and 67/33 PLA/TPU/PLA laminates showed proportionally lower UTS (25.4 and 20.0 MPa) but similar elongations (7.1–7.6 %), consistent with the diminished load transfer observed when the rigid phase becomes discontinuous (Cao et al., 2024). Apparent tensile moduli ranged from 471 to 625 MPa, values typical for rigid–soft laminates, though technique-dependent owing to crosshead-based strain measurement.

For TPU-faced laminates (TPU/PLA/TPU, 0.2 mm), the same pattern was observed but with slightly reduced strength relative to the PLA-faced counterparts. The 67/33 TPU/PLA/TPU laminate reached 31.2 MPa UTS and 6.9 % elongation, approximately 7 % below the equivalent PLA-faced design. The 50/50 and 33/67 stacks yielded 26.0 and 21.2 MPa UTS with elongations of 6.3 % and 5.6 %, respectively. This consistent reduction highlights the influence of outer-layer rigidity: PLA skins suppress strain localisation and delay necking, whereas compliant TPU surfaces deform early, initiating stress decay. Similar surface-dependence has been noted in previous studies (Shi et al., 2021) and (Brancewicz-Steinmetz et al., 2021).

Layer thickness, stacking sequence, and interface count were not independently varied. All PLA-faced samples used 0.1 mm layers (~60 layers total), while TPU-faced samples used 0.2 mm (~30 layers). Observed differences reflect coupled geometric and compositional effects. The single-material results confirmed that thicker layers improve UTS through improved interlayer diffusion (Wang et al., 2022), but within the laminates, composition and surface identity exerted a stronger influence than thickness alone.

Across all hybrid configurations, elongation at break remained between 5 % and 8 %, intermediate between PLA and TPU baselines. This range indicates partial strain transfer across the PLA–TPU interface, sufficient to prevent delamination but insufficient for full strain compatibility. Comparable constrained elongations (≈ 5–10 %) have been reported for co-moulded or dual-extrusion PLA–TPU systems (Feng & Ye, 2011; Rahmatabadi et al., 2022). The absence of abrupt failure or interfacial separation confirms adequate adhesion under optimised parameters, though residual stiffness mismatch and imperfect interdiffusion remain the limiting factors, as widely reported in other MMAM FDM studies (Allum et al., 2020; Brancewicz-Steinmetz et al., 2021).

3.3 Failure Modes and Interfacial Behaviour

Fracture morphology varied markedly with material configuration, reflecting the contrasting deformation mechanisms of PLA and TPU and the stress-transfer limits within the laminates. PLA specimens fractured abruptly with smooth, perpendicular surfaces and no necking, typical of brittle failure governed by limited chain mobility (Nofar et al., 2020; Wang et al., 2022). TPU specimens, by contrast, showed pronounced necking and whitening from stress-induced fibrillation and cavitation, followed by gradual rupture after significant thinning, evidence of highly ductile behaviour (Feng & Ye, 2011; Wilińska et al., 2025). The fracture morphology of representative specimens is shown in **Figure 9**.

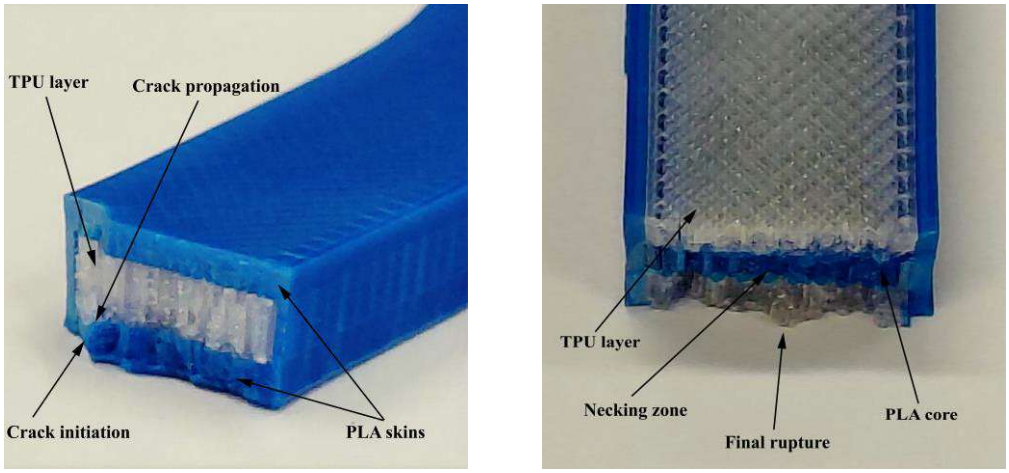

Figure 9. post-fracture tensile specimens **(a)** PLA/TPU/PLA showing crack initiation at the lower edge and crack propagation adjacent to the PLA–TPU interface (mixed-mode tearing), and **(b)** TPU/PLA/TPU showing pronounced TPU necking followed by final rupture

In the layered composites, cracks initiated near the PLA–TPU boundary where stiffness mismatch created local stress concentrations. Macroscopic inspection displayed propagation along or adjacent to this interface, indicating partial debonding but continuous load transfer (Brancewicz-Steinmetz et al., 2021; Rahmatabadi et al., 2022). PLA-faced laminates failed by brittle cracking of the outer PLA and ductile tearing of the TPU core, producing mixed-mode fracture typical of rigid–soft FDM systems (Cao et al., 2024; Shi et al., 2021). Minor peeling suggests incomplete polymer interdiffusion without full delamination. TPU-faced laminates appeared to fail more gradually. Outer TPU skins necked extensively, redistributing stress but lowering overall strength (Hamidi et al., 2025). No catastrophic separation occurred. All laminates remained partially bonded after fracture, confirming adequate interlayer adhesion for load sharing until failure consistent with adhesion performance in dual-nozzle FDM

(Brancewicz-Steinmetz et al., 2022; Cao et al., 2024). Uniform fracture features across replicates and low UTS scatter (± 1.2 MPa) indicate reproducible bonding quality.

Overall, fracture reflects brittle cracking in PLA, ductile tearing in TPU, and interfacial shear separation. Bonding strength was sufficient to prevent delamination but inadequate to homogenise deformation, identifying the PLA–TPU interface as the primary limitation to composite toughness and isotropy (Allum et al., 2020; Rahmatabadi et al., 2022).

4. Discussion

4.1 Mechanical contrast between PLA and TPU

The baseline tensile results confirm the extreme disparity in mechanical response between the two feedstocks. PLA is stiff and brittle while TPU is soft and highly extensible .This contrast mirrors the molecular architectures of a semi-crystalline aliphatic polyester and a segmented thermoplastic elastomer. Comparable values have been reported for FDM-printed PLA in both materials indicates improved filament diffusion and reduced porosity, supporting previous observed neck-growth mechanism (Wang et al., 2022).

4.2 Composition-dependent performance of laminates

The layered PLA–TPU composites exhibited mechanical properties intermediate between their constituents, governed primarily by the relative fraction and identity of the outer layers. The 67/33 PLA/TPU/PLA laminate reached 33.5 MPa and 7.7 % elongation approximately 70-80% of neat-PLA strength while doubling its ductility. This balance is consistent with nonlinear increases in toughness at higher TPU contents, attributed to plastic stress redistribution within the soft phase (Rahmatabadi et al., 2022). The reduction in strength with decreasing PLA fraction (to 20–25 MPa at 33/67–50/50) matches the percolation-type behaviour reported for melt-blended systems (Hamidi et al., 2025).

The modest difference between PLA-faced and TPU-faced laminates (typically ± 5–8 %) demonstrates that outer-layer stiffness influences load transfer but cannot fully compensate for interfacial weakness. PLA-faced stacks carried higher peak stresses when PLA formed a continuous outer shell, as stiff surface layers can limit strain localisation and delay the onset of interfacial shear failure (Brancewicz-Steinmetz et al., 2021). Conversely, TPU-faced specimens displayed smoother stress–strain curves and extended plastic zones, implying more homogeneous deformation but reduced load capacity.

4.3 Interfacial bonding and fracture mechanisms

Fracture analysis indicates that failure in all laminates was dominated by the PLA–TPU interface. The mixed-mode surfaces brittle PLA separation coupled with ductile tearing of TPU confirm that adhesion was sufficient to maintain load transfer until failure but not strong enough to enforce strain compatibility. Partial delamination traces correspond to limited molecular diffusion across the boundary, a known consequence of viscosity and surface-energy mismatch between PLA ($\gamma \approx 40$ mJ m^{-2}) and TPU ($\gamma \approx 30$ mJ m^{-2}) (Brancewicz-Steinmetz et al., 2021). Comparable interfacial failure patterns have been reported and are commonly attributed to insufficient interphase entanglement during extrusion (Shi et al., 2021) (Cao et al., 2024).

The absence of catastrophic separation despite interfacial cracking implies that mechanical interlocking, formed by partial wetting and surface roughness, contributed to adhesion. Similar observations indicate that, even without chemical compatibilisers, PLA–TPU interfaces can sustain several MPa of shear stress before debonding (Rahmatabadi et al., 2022). The present results support that conclusion. All laminates maintained structural integrity until failure, and UTS scatter (± 1.2 MPa) remained low, indicating consistent interface formation.

4.4 Effect of processing geometry

Because layer thickness and stacking sequence were not independently varied, their effects are inter-coupled. The trend of slightly higher UTS at 0.2 mm corroborates the layer-height effect observed for monolithic specimens, but within the laminates, the dominant variables are composition and surface identity. The data suggest that beyond a threshold of interfacial diffusion, additional geometric refinement (e.g., thinner layers) offers limited benefit unless accompanied by chemical or thermal surface activation. This aligns with previous work that achieved substantial toughness gains only when interface chemistry was modified or interlayer temperature was increased (Brancewicz-Steinmetz et al., 2022; Cao et al., 2024).

4.5 Broader implications

Overall, the study demonstrates that dual-extrusion FDM can reproducibly fabricate layered PLA–TPU composites with controllable mechanical balance, but interfacial adhesion remains the limiting factor in achieving isotropic strength and high toughness. Future optimisation should therefore target improved interphase diffusion via controlled pre-heating, compatibilisers, or surface activation to move beyond mechanically interlocked interfaces toward genuine co-bonded junctions.

5.0 Limitations and Recommendation

This study was limited by its macroscopic focus and coupled process parameters. Interfacial behaviour was inferred from tensile response and fracture morphology, as no microscopic or spectroscopic analyses were conducted to directly quantify polymer diffusion or bonding chemistry. Consequently, interpretations of adhesion quality are indirect. Layer thickness, stacking sequence, and interface count were varied simultaneously, preventing the independent assessment of geometric and compositional effects. Strain was derived from crosshead displacement, which underestimates true elongation once local necking or grip compliance occurs particularly for TPU and laminate specimens, so the reported ductility values represent conservative estimates. The use of a single grade of PLA and TPU also constrains material generalisation, while all tests were performed under controlled, dry, room-temperature conditions. These factors do not undermine the observed mechanical trends but indicate that future work should incorporate microscopic characterisation, decoupled parametric testing, and environmental loading to more fully resolve interfacial mechanisms in PLA–TPU composites.

6.0 Conclusion

This study performed a preliminary characterisation of the mechanical performance and interfacial behaviour of FDM composites produced from PLA and TPU, demonstrating how composition, layer sequence, and processing geometry govern tensile response. The results confirmed the pronounced mechanical contrast between the two base polymers. PLA provided high strength and stiffness but failed in a brittle manner, while TPU was highly ductile. Layered laminates exhibited intermediate behaviour, demonstrating that property balance can be tailored through material ratio and surface identity. The 67/33 PLA/TPU/PLA configuration achieved the optimum combination of strength (33.5 MPa) and ductility (7.7 %), representing approximately 72 % of PLA strength with a twofold increase in strain to failure.

Visual fracture analysis showed that failure consistently initiated at or near the PLA–TPU interface, producing mixed brittle–ductile fracture with partial delamination but no catastrophic separation. This indicates that mechanical interlocking and limited diffusion bonding were sufficient for load sharing, though interfacial adhesion remained the primary factor limiting toughness and isotropy. The low scatter in UTS (± 1.2 MPa) demonstrates that dual-extrusion FDM can reproducibly fabricate MMAM composites with consistent interfacial quality.

Overall, the findings show that mechanical performance in PLA–TPU systems is dominated by interfacial and architectural factors rather than layer thickness alone. Achieving further improvements will require strategies that promote interphase diffusion or chemical

compatibility, such as thermal surface activation, compatibiliser addition, or controlled pre-heating. Future work should also employ microscopic and spectroscopic characterisation to directly quantify interfacial bonding and investigate long-term environmental durability.

Acknowledgement

The authors would like to thank the University of Sunderland for its support, and laboratory technician David Winter for his assistance with sample preparation.

Credit Author Statement

Methodology, A.R. and N.N.; Investigation, A.R. and N.N.; Analysis, M.A.; Writing, original draft, M.A.; Writing, review and editing, M.A., A.R. and N.N.; Supervision, NN. and M.A.; All authors have read and agreed to the published version of the manuscript.

Conflicts of Interest

The authors declare no conflict of interest.

Artificial Intelligence (AI) Transparency Statement

Artificial intelligence tools ChatGPT 5.0 were used only to enhance grammar, clarity, and manuscript readability. They were not used to generate, analyse, or interpret data, nor to create scientific hypotheses, conclusions, or literature reviews. All content remains the intellectual product of the authors. Any AI-assisted text was carefully checked, revised, and validated to ensure compliance with research integrity and publisher guidelines.

References

Abidaryan, S., Akoundi, B., & Hajami, F. (2022). Additive manufacturing and investigation of shape memory properties of polylactic acid/thermoplastic polyurethane blend. *Journal of Elastomers and Plastics*. https://doi.org/10.1177/00952443221147028

Ahad, N. A. (2020). A Recent blend of thermoplastic polyurethane (TPU). *IOP Conference Series: Materials Science and Engineering*, *957*(1), 012045. https://doi.org/10.1088/1757-899X/957/1/012045

Allum, J., Moetazedian, A., Gleadall, A., & Silberschmidt, V. V. (2020). Interlayer bonding has bulk-material strength in extrusion additive manufacturing: New understanding of anisotropy. *Additive Manufacturing*, *34*, 101297. https://doi.org/10.1016/j.addma.2020.101297

Arruda, E. M., & Boyce, M. C. (1993). A three-dimensional constitutive model for the large stretch behavior of rubber elastic materials. *Journal of the Mechanics and Physics of Solids*, *41*(2), 389–412. https://doi.org/10.1016/0022-5096(93)90013-6

ASTM D638. (2022). Standard Test Method for Tensile Properties of Plastics. In *ASTM Standards*. ASTM International. https://doi.org/10.1520/D0638-14

Brancewicz-Steinmetz, E., Sawicki, J., & Byczkowska, P. (2021). The influence of 3d printing parameters on adhesion between polylactic acid (Pla) and thermoplastic polyurethane (tpu). *Materials*, *14*(21). https://doi.org/10.3390/ma14216464

Brancewicz-Steinmetz, E., Vergara, R. D. V., Buzalski, V. H., & Sawicki, J. (2022). Study of the adhesion between TPU and PLA in multi-material 3D printing. *Journal of Achievements in Materials and Manufacturing Engineering*, *115*(2), 49–56. https://doi.org/10.5604/01.3001.0016.2672

Cao, A., Wan, D., Gao, C., & Elverum, C. W. (2024). A novel method of fabricating designable polylactic acid (PLA)/thermoplastic polyurethane (TPU) composite filaments and structures by material extrusion additive manufacturing. *Journal of Manufacturing Processes*, *118*, 432–447. https://doi.org/10.1016/j.jmapro.2024.03.015

Darnal, A., Shahid, Z., Deshpande, H., Kim, J., & Muliana, A. (2023). Tuning mechanical properties of 3D printed composites with PLA:TPU programmable filaments. *Composite Structures*, *318*, 117075. https://doi.org/10.1016/j.compstruct.2023.117075

Elmrabet, N., & Siegkas, P. (2020). Dimensional considerations on the mechanical properties of 3D printed polymer parts. *Polymer Testing*, *90*, 106656. https://doi.org/10.1016/j.polymertesting.2020.106656

Feng, F., & Ye, L. (2011). Morphologies and mechanical properties of polylactide/thermoplastic polyurethane elastomer blends. *Journal of Applied Polymer Science*, *119*(5), 2778–2783. https://doi.org/10.1002/app.32863

García-Collado, A., Blanco, J. M., Gupta, M. K., & Dorado-Vicente, R. (2022). Advances in polymers based Multi-Material Additive-Manufacturing Techniques: State-of-art review on properties and applications. In *Additive Manufacturing* (Vol. 50, p. 102577). Elsevier. https://doi.org/10.1016/j.addma.2021.102577

Hamidi, M. N., Abdullah, J., Mahmud, A. S., Hassan, M. H., & Zainoddin, A. Y. (2025). Influence of thermoplastic polyurethane (TPU) and printing parameters on the thermal and mechanical performance of polylactic acid (PLA) / thermoplastic polyurethane (TPU) polymer. *Polymer Testing*, *143*, 108697. https://doi.org/10.1016/j.polymertesting.2025.108697

Hasanov, S., Alkunte, S., Rajeshirke, M., Gupta, A., Huseynov, O., Fidan, I., Alifui-Segbaya, F., & Rennie, A. (2022). Review on additive manufacturing of multi-material parts: Progress and challenges. In *Journal of Manufacturing and Materials Processing* (Vol. 6, Issue 1, p. 4). Multidisciplinary Digital Publishing Institute. https://doi.org/10.3390/jmmp6010004

Mi, H. Y., Salick, M. R., Jing, X., Jacques, B. R., Crone, W. C., Peng, X. F., & Turng, L. S. (2013). Characterization of thermoplastic polyurethane/polylactic acid (TPU/PLA) tissue engineering scaffolds fabricated by microcellular injection molding. *Materials Science and Engineering C*, *33*(8), 4767–4776. https://doi.org/10.1016/j.msec.2013.07.037

Nasution, A., Herianto, Rifai, A. P., & Atsani, S. I. (2025). Tensile performance of multi-material sandwich structures fabricated by multi-nozzle fused deposition modeling using PLA, ABS, and HIPS. *Results in Engineering*, *27*, 106210. https://doi.org/10.1016/J.RINENG.2025.106210

Naveed, N., Anwar, M. N., Armstrong, M., Ahmad, F., Irfan Ul Haq, M., & Ridley, G. (2025). Enhancing Sustainability and Functionality with Recycled Materials in Multi-Material Additive Manufacturing. *Sustainability (Switzerland)*, *17*(13).

https://doi.org/10.3390/su17136105

Nazir, A., Gokcekaya, O., Md Masum Billah, K., Ertugrul, O., Jiang, J., Sun, J., & Hussain, S. (2023). Multi-material additive manufacturing: A systematic review of design, properties, applications, challenges, and 3D printing of materials and cellular metamaterials. In *Materials and Design* (Vol. 226, p. 111661). Elsevier. https://doi.org/10.1016/j.matdes.2023.111661

Nofar, M., Mohammadi, M., & Carreau, P. J. (2020). Effect of TPU hard segment content on the rheological and mechanical properties of PLA/TPU blends. *Journal of Applied Polymer Science*, *137*(45), 49387. https://doi.org/10.1002/app.49387

Omer, M. A. E., Shaban, I. A., Mourad, A. H., & Hegab, H. (2025). Advances in interlayer bonding in fused deposition modelling: a comprehensive review. In *Virtual and Physical Prototyping* (Vol. 20, Issue 1, p. 2522951). Taylor and Francis Ltd. https://doi.org/10.1080/17452759.2025.2522951

Plotzke, J. J., Torgerson, N. R., Seaberg, S. D., & McClain, M. S. (2024). Mechanical Properties of 3D-Printed Multi-Material Polymeric Composites. *AIAA SciTech Forum and Exposition, 2024*. https://doi.org/10.2514/6.2024-1225

Qi, H. J., & Boyce, M. C. (2005). Stress-strain behavior of thermoplastic polyurethanes. *Mechanics of Materials*, *37*(8), 817–839. https://doi.org/10.1016/j.mechmat.2004.08.001

Rahmatabadi, D., Ghasemi, I., Baniassadi, M., Abrinia, K., & Baghani, M. (2022). 3D printing of PLA-TPU with different component ratios: Fracture toughness, mechanical properties, and morphology. *Journal of Materials Research and Technology*, *21*, 3970–3981. https://doi.org/10.1016/j.jmrt.2022.11.024

Ranakoti, L., Gangil, B., Mishra, S. K., Singh, T., Sharma, S., Ilyas, R. A., & El-Khatib, S. (2022). Critical Review on Polylactic Acid: Properties, Structure, Processing, Biocomposites, and Nanocomposites. *Materials*, *15*(12), 4312. https://doi.org/10.3390/MA15124312

Shi, X., Chen, B., Tuo, X., Gong, Y., & Guo, J. (2021). Study on performance characteristics of fused deposition modeling 3D-printed composites by blending and lamination. *Journal of Applied Polymer Science*, *138*(9), 32495. https://doi.org/10.1002/app.49926

Tamburrino, F., Graziosi, S., & Bordegoni, M. (2019). The influence of slicing parameters on

the multi-material adhesion mechanisms of FDM printed parts: an exploratory study. *Virtual and Physical Prototyping*, *14*(4), 316–332. https://doi.org/10.1080/17452759.2019.1607758

Wang, F., Ji, Y., Chen, C., Zhang, G., & Chen, Z. (2022). Tensile properties of 3D printed structures of polylactide with thermoplastic polyurethane. *Journal of Polymer Research*, *29*(8). https://doi.org/10.1007/s10965-022-03172-6

Wilińska, K., Kozuń, M., & Pezowicz, C. (2025). Elastic Properties of Thermoplastic Polyurethane Fabricated Using Multi Jet Fusion Additive Technology. *Polymers*, *17*(10). https://doi.org/10.3390/polym17101363

Yin, J., Lu, C., Fu, J., Huang, Y., & Zheng, Y. (2018). Interfacial bonding during multi-material fused deposition modeling (FDM) process due to inter-molecular diffusion. *Materials and Design*, *150*, 104–112. https://doi.org/10.1016/j.matdes.2018.04.029